Thin-Walled Structures 96 (2015) 286–294

Contents lists available at ScienceDirect

Thin-Walled Structures

journal homepage: www.elsevier.com/locate/tws

Equatorial bending of an elliptic toroidal shell

Alphose Zingoni *, Nosakhare Enoma, Nishalin Govender

Department of Civil Engineering, University of Cape Town, Rondebosch 7701, Cape Town, South Africa

ARTICLE INFO

Article history:
Received 5 August 2015
Received in revised form
18 August 2015
Accepted 18 August 2015

Keywords:
Toroidal shell
Elliptic toroid
Shell of revolution
Bending theory of shells
Shell analysis
Discontinuity stresses
Containment vessel

ABSTRACT

The exact differential equations for the axisymmetric bending of elliptic toroidal shells are difficult to solve. In this paper, and by considering a semi-elliptic toroid, we present an approximate bending solution that is valid in regions adjacent to the horizontal equatorial plane. The formulation accurately simulates edge effects which may arise from loading and geometric discontinuities located in the equatorial plane of elliptic toroids. In particular, the developed closed-form results provide a very effective means for evaluating the state of stress in the relatively narrow zones experiencing mid-side local effects in complete elliptic toroidal vessels subjected to hydrostatic loading, and for calculating the deformed shape of the shell midsurface.

1. Introduction

The membrane theory of shells is a greatly simplified yet very effective basis for estimating stresses and deformations in those regions of the shell over which the loading and geometry do not change too rapidly. However, and as is well-known, the theory becomes inadequate at or in the vicinity of supports, concentrated loadings, shell junctions or discontinuities in shell geometry (thickness, slope, radii of curvature), loading and material properties. Novozhilov [1] has called these locations "lines of distortion" in reference to the existence of a bending effect locally disturbing the membrane state of stress in these regions. Discontinuity problems in shells of revolution have been the subject of many investigations, and a good body of closed-form results exists for the more common types of shells and loading conditions [2–5].

The performance of containment shells is usually assessed with regard to their stress and deformation response in the linear elastic range [2,3], their vibration characteristics and dynamic response, as well as their nonlinear buckling and postbuckling behaviour within the elastic and plastic ranges of material behaviour. Metal shells are particularly susceptible to buckling on account of their thin-ness (radius-to-thickness ratios typically in excess of 500). Numerical studies have been carried out on the buckling capacity of vertical cylindrical steel tanks [6–11], horizontal cylindrical and near-cylindrical vessels [12–14] and conical tanks [15–17]. The buckling capacity of multi-segmented shells under external water pressurisation has also been investigated [18], as has the elastic buckling of certain unusual mathematical forms for shells [19,20].

Junction stresses in various shell assemblies and multi-segmented vessels have been the subject of intensive studies over the past 15 years [21–25]. Mechanics phenomena around shell intersections and at shell-branching locations have also been of interest [26,27]. The presence of ring beams at shell junctions has a considerable influence on the behaviour of the shell; some efforts have also been directed towards understanding ring–shell interactions [28,29]. A more comprehensive review of recent studies on the statics, dynamics and stability of various types of liquid-containment shells under a variety of loading conditions may be seen in a recent survey [30].

Toroidal shells have mostly been studied with pressure-vessel applications in mind, though liquid-containment applications have also been of interest. The classical solutions for pressurised circular and elliptical toroids may be seen in texts on linear shell analysis [2–5]. Even where toroidal shells with uniform geometry are subjected to internal pressure only, the membrane solution becomes inadequate in the vicinity of the horizontal circles furthest from the equatorial plane, owing to the vanishing of the curvature in one of the principal planes [31].

Sutcliffe [32] tackled the stress analysis of both circular and elliptical toroidal shells subjected to internal pressure. While accurate for the purpose, the formulation is somewhat cumbersome

* Corresponding author. Fax: +27 21 650 3293.
E-mail address: alphose.zingoni@uct.ac.za (A. Zingoni).

http://dx.doi.org/10.1016/j.tws.2015.08.017
0263-8231/

for practical implementation. Galletly [33] considered the elastic buckling of an elliptic toroidal shell subjected to uniform internal pressure, and confirmed that internally pressurised elliptical toroids, unlike circular toroids, may possibly buckle, depending on the axes ratio of the elliptical cross-section. The study was also extended to plastic buckling [34], for which the post-buckling behaviour of the shell was noted to be stable.

Redekop [35] studied the buckling behaviour of an orthotropic toroidal shell of elliptical cross-section, while Yamada et al. [36] considered the free vibration response of a toroidal shell of elliptic section. Xu and Redekop [37] also considered the free vibration of elliptic toroidal shells, but with orthotropic properties. Zhan and Redekop [38] studied toroidal tanks with cross-sections made up of combinations of circular arcs of different radii (ovaloid shape), and observed the vibration, buckling and collapse behaviour of this type of toroidal vessel.

In this paper, we will focus attention on the thin elliptic toroidal shell. Noting the lack of a convenient analytical solution for the axisymmetric bending of an elliptic toroidal shell, we aim at developing a practical means for estimating bending-disturbance effects that may arise in the mid-side locations (herein referred to as "equatorial" locations) of vertically elongated thin elliptic toroids, where the vertical semi-axis b of the ellipse is greater than the horizontal semi-axis a. Specifically, we aim to develop and present a set of closed-form expressions for interior shell stresses due to axisymmetric bending moments and shearing forces applied in the equatorial plane of the elliptic section as uniformly distributed edge actions.

The formulation is intended for use in quantifying (i) the junction effects in the vicinity of the equatorial plane of subsea elliptic–toroidal shell structures (where a horizontal plate deck may be attached to the inner walls of the toroid to provide an interior working platform extending right round the torus), or (ii) the edge effects in the vicinity of supports where the elliptic toroidal vessel is used as an elevated circular tank supported on closely-spaced vertical columns attached at both the intrados and extrados of the torus. The relatively weak edge effects associated with partial filling of the tank may also be quantified on the basis of this solution. We will begin by defining the geometry of the elliptic toroid.

2. Geometrical preliminaries

Fig. 1 shows the relevant geometrical parameters of an elliptic toroidal shell. To generate the torus, an ellipse of semi-axes a (horizontal) and b (vertical) is rotated about a vertical axis $Y-Y$ that lies at a distance A ($>a$) from the local vertical axis $y-y$ of the ellipse. The equatorial plane (horizontal plane of symmetry) is denoted by $E-E$. In what follows, we will take the generator curve (or meridian) of the toroidal shell as the ellipse to the left of the axis $Y-Y$. Let P be any point on the generator meridian. The radius of curvature of the ellipse at point P is denoted by r_1 and the corresponding centre of curvature by O_1. For the three-dimensional toroidal surface, there would be two principal radii of curvature (being the maximum and minimum values of curvature) at any given point P, and these occur in planes perpendicular to each other. The first principal radius of curvature of the toroidal surface at point P is the radius of curvature r_1 ($=PO_1$) of the generator ellipse at that point, while the second principal radius of curvature at point P, denoted by r_2, is equal to the distance PO_2, where O_2 is the point at which the surface normal at P intersects the axis of revolution $Y-Y$ of the torus.

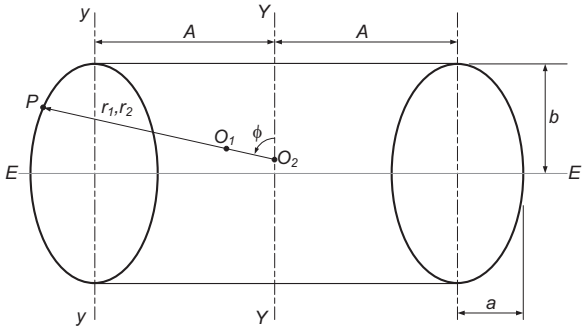

Fig. 1. Geometrical parameters of an elliptic toroidal shell.

Point P itself may be defined by an angular coordinate ϕ, which is the angle measured from the upward direction of the axis of revolution of the torus to the surface normal at point P. The range $0 \le \phi \le 2\pi$ covers all points on the toroidal surface, with $0 \le \phi \le \pi$ describing points in the outer region of the torus, and $\pi \le \phi \le 2\pi$ describing points in the inner region of the torus; the coordinates $\phi = \pi/2$ and $\phi = 3\pi/2$ define points on the equatorial plane, which of course correspond to the extrados and intrados of the torus with respect to the axis $Y-Y$.

For the outer region of the torus ($0 \le \phi \le \pi$), the principal radii of curvature are given by [3]

$$r_1 = \frac{a^2 b^2}{\left(a^2 \sin^2\phi + b^2 \cos^2\phi\right)^{3/2}} \text{ (positive)} \tag{1a}$$

$$r_2 = \frac{A}{\sin\phi} + \frac{a^2}{\left(a^2 \sin^2\phi + b^2 \cos^2\phi\right)^{1/2}} \text{ (positive)} \tag{1b}$$

while for the inner region ($\pi \le \phi \le 2\pi$), these become

$$r_1 = \frac{-a^2 b^2}{\left(a^2 \sin^2\phi + b^2 \cos^2\phi\right)^{3/2}} \text{ (negative)} \tag{2a}$$

$$r_2 = \frac{A}{|\sin\phi|} - \frac{a^2}{\left(a^2 \sin^2\phi + b^2 \cos^2\phi\right)^{1/2}} \text{ (positive)} \tag{2b}$$

The values of r_1 and r_2 at the extrados of the torus ($\phi = \pi/2$) and the intrados ($\phi = 3\pi/2$), which correspond to the outer and inner sides of the elliptical section, will be required in due course. Evaluating these, we obtain

$$r_1 = \frac{b^2}{a} \tag{3a}$$

$$r_2 = A + a \tag{3b}$$

at the extrados, and

$$r_1 = -\frac{b^2}{a} \tag{4a}$$

$$r_2 = A - a \tag{4b}$$

at the intrados.

3. Governing equation

Fig. 2 shows a bending element of an axisymmetrically-loaded shell of revolution in the $\{\phi, \theta\}$ coordinate system. Here, the meridional angle ϕ identifies the position of a point along a given

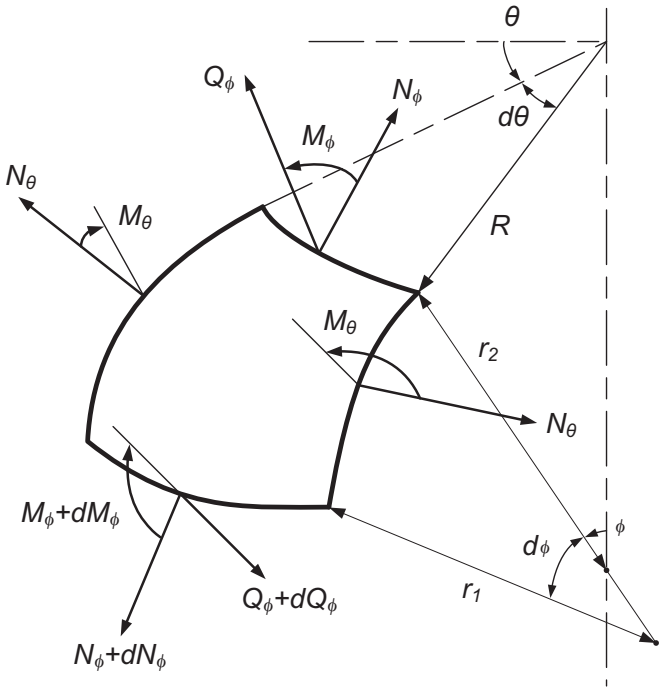

Fig. 2. Element of a shell of revolution under axisymmetric bending.

meridian of the shell (as already defined), while the coordinate θ is the circumferential angle measured from an arbitrary vertical plane to the vertical plane containing the meridian in question, the two vertical planes intersecting at the axis of revolution of the shell. The element is in equilibrium under the loads acting over its surface (external loading on the shell) and the forces and moments acting along its four edges (internal actions in the shell), but in the figure, the surface loading is not shown, since we will only be concerned with edge effects.

The actions $\{N_\phi,\ N_\theta\}$ are direct forces per unit length of the edge, acting in the direction of the tangent to the shell meridian at any given point (henceforth called the meridional direction), and the direction of the tangent to the horizontal circumferential circle passing through that point (henceforth called the hoop direction), respectively. The actions $\{M_\phi,\ M_\theta\}$ are bending moments per unit length of the edge, as seen in the vertical meridional section and the horizontal hoop section respectively. The action Q_ϕ is a shear force per unit length of the edge, acting in the meridional section; there is no shear force in the horizontal section ($Q_\theta = 0$), owing to axisymmetry. All meridional actions are shown incremented in the direction of increasing ϕ, but the hoop actions do not change with respect to θ owing to axisymmetry.

Considering equilibrium of the shell element, and making use of strain–displacement relations as well as Hooke's law, we may express N_ϕ, N_θ, M_ϕ and M_θ in terms of displacements, and then reduce the ensuing relationships to the well-known Reissner–Meissner differential equations for the axisymmetric bending of general shells of revolution [2,3]

$$\left[D\left(\frac{r_2}{r_1}\right)\sin\phi\right]\frac{d^2V}{d\phi^2}+\left[D\left(\frac{r_2}{r_1}\right)\cos\phi+\sin\phi\frac{d}{d\phi}\left(D\frac{r_2}{r_1}\right)\right]\frac{dV}{d\phi}$$
$$+\left[\nu\left(\cos\phi\frac{dD}{d\phi}-D\sin\phi\right)-D\left(\frac{r_1}{r_2}\right)\frac{\cos^2\phi}{\sin\phi}\right]V=-r_1r_2(\sin\phi)Q_\phi \tag{5a}$$

$$\frac{r_2^2}{tr_1}\frac{d^2Q_\phi}{d\phi^2}+\left[\frac{r_2^2}{tr_1}\cot\phi+\frac{r_2}{tr_1}\frac{dr_2}{d\phi}+\frac{d}{d\phi}\left(\frac{r_2^2}{tr_1}\right)\right]\frac{dQ_\phi}{d\phi}$$
$$+\left[\frac{r_2}{tr_1}\frac{d^2r_2}{d\phi^2}+\left\{\frac{d}{d\phi}\left(\frac{r_2}{tr_1}\right)\right\}\frac{dr_2}{d\phi}\right.$$
$$\left.+\left\{\left(\frac{r_2+\nu r_1}{r_1}\right)\frac{dr_2}{d\phi}-(r_1+\nu r_2)\cot\phi\right\}\frac{\cot\phi}{t}\right.$$
$$\left.-\nu\left\{(\cot\phi)\frac{d}{d\phi}\left(\frac{r_2}{t}\right)-\left(\frac{r_2}{t}\right)\frac{1}{\sin^2\phi}\right\}\right]Q_\phi=r_1EV \tag{5b}$$

In these equations, the variable V is the angular rotation of the shell meridian as seen in the meridional section, while Q_ϕ is the shear force as already defined. The material properties E (Young's modulus of elasticity) and ν (Poisson's ratio) are assumed to be constant. The parameter t denotes shell thickness, while D is the flexural rigidity of the shell, given by

$$D=\frac{Et^3}{12(1-\nu^2)} \tag{6}$$

For thin shells of revolution which are not shallow (non-shallow shells shall be taken as those in which bending phenomena occur in locations for which ϕ is at least $\pi/6$ from the locations $\phi = 0$ and $\phi = \pi$), second-derivative terms of V and Q_ϕ are much bigger than first-derivative and zero-derivative terms. As an approximation, we may therefore drop all first-derivative and zero-derivative terms on the left-hand sides of Eqs. (5), so that the equations become

$$\frac{d^2V}{d\phi^2}=-\frac{r_1^2}{D}Q_\phi \tag{7a}$$

$$\frac{d^2Q_\phi}{d\phi^2}=\frac{r_1^2}{r_2^2}\ EtV \tag{7b}$$

In the present problem of the prolate (vertically-elongated) elliptical cross-section ($b > a$), this approximation is particularly justified, since we intend to investigate bending phenomena in regions that are adjacent to the equatorial plane ($\phi = \pm\pi/2$), where the sides of the elliptical section remain fairly steep for a considerable distance on either side of the equatorial plane.

Combining Eqs. (7a) and (7b), we obtain the fourth-order differential equation

$$\frac{d^4Q_\phi}{d\phi^4}+4\lambda^4Q_\phi=0 \tag{8}$$

where λ is a slenderness parameter defined as follows:

$$\lambda^4=\frac{r_1^4Et}{4Dr_2^2}=3\left(1-\nu^2\right)\frac{r_1^4}{r_2^2t^2} \tag{9}$$

For the elliptical toroidal shell, the principal radii of curvature r_1 and r_2 are functions of ϕ (as given by Eqs. (1) and (2)), so the slenderness parameter λ is also a function of ϕ, implying that the second term of the above fourth-order differential equation has a variable coefficient. Given the complexity of this coefficient, the exact solution of Eq. (8) is rather difficult to obtain.

4. Approximate general solution

Now for a prolate elliptical profile, the radii of curvature r_1 and r_2 vary rather slowly in the neighbourhoods of the equatorial

plane, which are the regions of present interest. Based on this observation, we will introduce the further approximation that r_1 and r_2 are practically constant in the narrow zones adjacent to the equatorial plane and within which bending disturbances are confined. These constant values of r_1 and r_2 will be taken as the values at the location $\phi = \pi/2$ (for the outer part of the toroidal shell) and the location $\phi = 3\pi/2$ (for the inner part of the toroidal shell), as already given by Eqs. (3) and (4).

With this simplification, the slenderness parameter λ in Eq. (9) is now a constant, and the fourth-order differential equation (Eq. (8)) now has constant coefficients. This allows us to take the general solution of Eq. (8) in the well-known form [3]

$$Q_\phi = e^{\lambda\phi}(C_1 \cos\lambda\phi + C_2 \sin\lambda\phi) + e^{-\lambda\phi}(C_3 \cos\lambda\phi + C_4 \sin\lambda\phi) \tag{10}$$

where C_1, C_2, C_3 and C_4 are constants of integration to be evaluated from the boundary conditions of the shell. Based on the well-known behaviour of spherical and cylindrical shells, let us tentatively assume that for the semi-elliptical toroidal shell, the bending disturbance emanating from either the outer edge or the inner edge is of a decaying character. Furthermore, let us assume that any adjacent edges of the shell are sufficiently far apart to allow decoupling of edge effects. This permits us to retain only two of the constants appearing in Eq. (10), and to rewrite the solution as

$$Q_\phi = Ce^{-\lambda\psi} \sin(\lambda\psi + \beta) \tag{11}$$

where ψ is now the meridional angle measured from the normal at the edge of the shell to the normal at the point in question; C and β are new constants of integration. For the shell edge located in the equatorial plane, the relationship between ϕ and ψ is simply

$$\psi = \frac{\pi}{2} - \phi; \quad \psi = \phi - \frac{3\pi}{2} \tag{12a, b}$$

where the first equation refers to the outer edge of the semi-elliptic toroidal shell, and the second refers to the inner edge (closer to the axis of revolution).

Equilibrium considerations of the shell element yield

$$N_\phi = -Q_\phi \cot\phi \approx 0 \tag{13}$$

since $\cot\phi \approx 0$ in the vicinity of the toroidal shell edges ($\phi = \pi/2;\ 3\pi/2$). For the hoop stress resultant, we obtain,

$$N_\theta = -\left(\frac{r_2}{r_1}\frac{dQ_\phi}{d\phi} + \frac{1}{r_1}\frac{dr_2}{d\phi}Q_\phi\right) \approx -\frac{r_2}{r_1}\frac{dQ_\phi}{d\phi} \tag{14}$$

ignoring the second term in Q_ϕ in relation to the first term in the first derivative of Q_ϕ, particularly as the rate of variation of r_2 with respect to ϕ is also very small in the neighbourhood of the equatorial plane.

In evaluating the edge effects, compatibility conditions involving the horizontal displacement δ of the shell edge (which is a movement perpendicular to the axis of revolution of the torus), and the meridional rotation V of the shell edge, will be required. From Eq. (7b), we may write V as follows:

$$V = \frac{1}{Et}\left(\frac{r_2^2}{r_1^2}\right)\frac{d^2Q_\phi}{d\phi^2} \tag{15}$$

From strain–displacement and stress–strain considerations, the horizontal displacement δ may be expressed in terms of the stress resultants N_ϕ and N_θ as follows:

$$\delta = \frac{1}{Et}(r_2 \sin\phi)(N_\theta - \nu N_\phi) \approx \frac{1}{Et}(r_2 \sin\phi)N_\theta \tag{16}$$

since $N_\phi \approx 0$. Using result (14) to eliminate N_θ, we obtain

$$\delta \approx -\frac{1}{Et}(r_2 \sin\phi)\left(\frac{r_2}{r_1}\right)\frac{dQ_\phi}{d\phi} \tag{17}$$

Using curvature–rotation relations and Hooke's law, the bending moment M_ϕ may be expressed in terms of the rotation V as follows:

$$M_\phi = -D\left\{\frac{1}{r_1}\frac{dV}{d\phi} + \frac{\nu}{r_2}V\cot\phi\right\} \approx -D\left(\frac{1}{r_1}\right)\frac{dV}{d\phi} \tag{18}$$

neglecting the second term (in V) in relation to the first term (in the first derivative of V), particularly as the second term also contains the factor $\cot\phi$ (≈ 0 in the neighbourhood of the equatorial plane). Making use of Eq. (15) to eliminate V, and using the approximation that, for the prolate elliptical profile, r_2 and r_1 are practically constant in the narrow zone experiencing edge effects, we obtain

$$M_\phi \approx -\frac{D}{Etr_1}\left(\frac{r_2^2}{r_1^2}\right)\frac{d^3Q_\phi}{d\phi^3} \tag{19}$$

Similarly,

$$M_\theta = -D\left\{\frac{1}{r_2}V\cot\phi + \frac{\nu}{r_1}\frac{dV}{d\phi}\right\} \approx -D\left(\frac{\nu}{r_1}\right)\frac{dV}{d\phi} \approx \nu M_\phi \tag{20}$$

(neglecting the first term in relation to the second).

At this stage, we may now make use of the general solution for Q_ϕ (Eq. (11)) to eliminate Q_ϕ from the above relationships. The results are as follows:

$$N_\phi \approx 0 \tag{21}$$

$$N_\theta \approx C\lambda\left(\frac{r_2}{r_1}\right)e^{-\lambda\psi}\{\cos(\lambda\psi + \beta) - \sin(\lambda\psi + \beta)\} \tag{22}$$

$$M_\phi \approx \frac{2\lambda^3 D}{Etr_1}\left(\frac{r_2^2}{r_1^2}\right)Ce^{-\lambda\psi}\{\cos(\lambda\psi + \beta) + \sin(\lambda\psi + \beta)\} \tag{23}$$

$$M_\theta \approx \nu M_\phi \tag{24}$$

$$\delta \approx \frac{C\lambda}{Et}\left(\frac{r_2}{r_1}\right)(r_2 \sin\phi)\, e^{-\lambda\psi}\{\cos(\lambda\psi + \beta) - \sin(\lambda\psi + \beta)\} \tag{25}$$

$$V \approx -\frac{2C\lambda^2}{Et}\left(\frac{r_2^2}{r_1^2}\right)e^{-\lambda\psi}\cos(\lambda\psi + \beta) \tag{26}$$

5. Boundary conditions and generalised edge effects

Fig. 3 shows the edges of the semi-elliptical toroidal shell subjected to uniformly distributed bending moments and horizontal shearing forces, where $\{M_{e1},\ H_{e1}\}$ are the axisymmetric actions applied at the outer edge, and $\{M_{e2},\ H_{e2}\}$ are the axisymmetric actions applied at the inner edge. The following treatment applies equally to the two edges. In the formulation, we

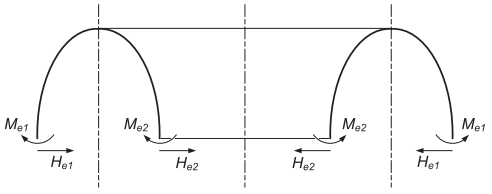

Fig. 3. Bending and shearing edge actions on a semi-elliptic toroidal shell.

will therefore denote the applied edge bending moments and edge shearing forces simply by M_e and H_e, with ψ denoting the meridional angle from the edge in question (outer or inner).

When M_e only is applied at a given edge (in the absence of H_e), we want to choose the constants C and β such that the following boundary conditions are satisfied:

$$\left(M_\phi\right)_{\psi=0} = M_e \tag{27a}$$

$$\left(Q_\phi\right)_{\psi=0} = 0 \tag{27b}$$

Applying these conditions to Eqs. (11) and (23), we obtain

$$\beta = 0 \tag{28a}$$

$$C = \frac{Etr_1}{2\lambda^3 D}\left(\frac{r_1^2}{r_2^2}\right) M_e \tag{28b}$$

Substituting these values of β and C into Eqs. (21)–(26), we obtain the interior stress resultants, bending moments and deformations due to the edge bending moment M_e as follows:

$$N_\phi \approx 0 \tag{29}$$

$$N_\theta = \frac{Etr_1}{2\lambda^2 D}\left(\frac{r_1}{r_2}\right) e^{-\lambda\psi}(\cos\lambda\psi - \sin\lambda\psi) M_e \tag{30}$$

$$M_\phi = e^{-\lambda\psi}(\cos\lambda\psi + \sin\lambda\psi) M_e \tag{31}$$

$$M_\theta \approx \nu\, M_\phi \tag{32}$$

$$\delta = \left(\frac{r_1^2}{2\lambda^2 D}\right)(\sin\phi)\, e^{-\lambda\psi}(\cos\lambda\psi - \sin\lambda\psi) M_e \tag{33}$$

$$V = -\left(\frac{r_1}{\lambda D}\right) e^{-\lambda\psi}(\cos\lambda\psi) M_e \tag{34}$$

At the edge $(\psi = 0)$, we have

$$\delta_e = \left(\frac{r_1^2}{2\lambda^2 D}\right) M_e \tag{35}$$

$$V_e = -\left(\frac{r_1}{\lambda D}\right) M_e \tag{36}$$

When H_e only is applied at a given edge (in the absence of M_e), we want to choose the constants C and β such that the following boundary conditions are satisfied:

$$\left(M_\phi\right)_{\psi=0} = 0 \tag{37a}$$

$$\left(Q_\phi\right)_{\psi=0} = H_e \tag{37b}$$

Applying these conditions to Eqs. (11) and (23), we obtain

$$\beta = -\frac{\pi}{4} \tag{38a}$$

$$C = -\sqrt{2}\, H_e \tag{38b}$$

Substitution of these values of β and C into Eqs. (21)–(26) gives the interior stress resultants, bending moments and deformations due to the edge shear H_e as follows:

$$N_\phi \approx 0 \tag{39}$$

$$N_\theta = -2\lambda\left(\frac{r_2}{r_1}\right) e^{-\lambda\psi}(\cos\lambda\psi) H_e \tag{40}$$

$$M_\phi = -\frac{4\lambda^3 D}{Etr_1}\left(\frac{r_2^2}{r_1^2}\right) e^{-\lambda\psi}(\sin\lambda\psi) H_e \tag{41}$$

$$M_\theta \approx \nu\, M_\phi \tag{42}$$

$$\delta = -\frac{2\lambda}{Et}\left(\frac{r_2}{r_1}\right)(r_2 \sin\phi) e^{-\lambda\psi}(\cos\lambda\psi) H_e \tag{43}$$

$$V = \frac{2\lambda^2}{Et}\left(\frac{r_2^2}{r_1^2}\right) e^{-\lambda\psi}(\cos\lambda\psi + \sin\lambda\psi) H_e \tag{44}$$

At the edge $(\psi = 0)$, we have

$$\delta_e = -\frac{2\lambda}{Et}\left(\frac{r_2}{r_1}\right) r_2\, H_e \tag{45}$$

$$V_e = \frac{2\lambda^2}{Et}\left(\frac{r_2^2}{r_1^2}\right) H_e \tag{46}$$

6. Shell stresses due to edge actions

The bending-related shell stresses σ_ϕ (in the meridional direction) and σ_θ (in the hoop direction) are obtained by combining the direct stresses due to the stress resultants N_ϕ and N_θ (which are constant across the shell thickness) with the flexural stresses due to the bending moments M_ϕ and M_θ (which vary linearly across the shell thickness from a positive value on one side of the shell midsurface to a negative value of the same magnitude on the opposite side of the shell midsurface). Thus,

$$\sigma_\phi = \frac{N_\phi}{t} \pm \frac{6M_\phi}{t^2} \approx \pm\frac{6M_\phi}{t^2} \tag{47a}$$

$$\sigma_\theta = \frac{N_\theta}{t} \pm \frac{6M_\theta}{t^2} = \frac{N_\theta}{t} \pm \nu\left(\frac{6M_\phi}{t^2}\right) \tag{47b}$$

where the first equation makes use of the fact that $N_\phi \approx 0$ (Eqs. (29) and (39)) and the second equation makes use of the relationship $M_\theta \approx \nu M_\phi$ (Eqs. (32) and (42)). In the notation $\pm$, the upper sign refers to the inner surface of the shell (with respect to the *global* axis of revolution of the torus), while the lower sign refers to the outer surface.

For the stresses due to the edge bending moment M_e, we substitute the results for M_ϕ and N_θ (as given by Eqs. (30) and (31)) into the above expressions, and then eliminate the parameters D and λ using Eqs. (6) and (9) respectively, leading to the results:

$$\sigma_\phi = \pm\frac{6M_e}{t^2} e^{-\lambda\psi}(\cos\lambda\psi + \sin\lambda\psi) \tag{48a}$$

$$\begin{aligned}\sigma_\theta &= \frac{Er_1}{2\lambda^2 D}\left(\frac{r_1}{r_2}\right) M_e e^{-\lambda\psi}(\cos\lambda\psi - \sin\lambda\psi) \\ &\quad \pm \nu\frac{6M_e}{t^2} e^{-\lambda\psi}(\cos\lambda\psi + \sin\lambda\psi) \\ &= \frac{2M_e}{t^2} e^{-\lambda\psi}\left[\left\{3\left(1-\nu^2\right)\right\}^{1/2}(\cos\lambda\psi - \sin\lambda\psi)\right. \\ &\quad \left. \pm 3\nu\,(\cos\lambda\psi + \sin\lambda\psi)\right]\end{aligned} \tag{48b}$$

For the stresses due to the edge shearing force H_e, we substitute

the results for M_ϕ and N_θ (as given by Eqs. (40) and (41)) into relations (47), and then eliminate the parameters D and λ using Eqs. (6) and (9) respectively, leading to the results

$$\sigma_\phi = \mp \frac{24\lambda^3 D}{Et^3 r_1}\left(\frac{r_2^2}{r_1^2}\right)e^{-\lambda\psi}(\sin\lambda\psi)$$

$$H_e = \mp \frac{6H_e}{\left\{3\left(1-\nu^2\right)\right\}^{1/4}}\left(\frac{1}{t^{3/2}}\right)(r_2)^{1/2}e^{-\lambda\psi}\sin\lambda\psi \tag{49a}$$

$$\sigma_\theta = -\frac{2\lambda}{t}\left(\frac{r_2}{r_1}\right)e^{-\lambda\psi}(\cos\lambda\psi)H_e \mp \nu\frac{24\lambda^3 D}{Et^3 r_1}\left(\frac{r_2^2}{r_1^2}\right)e^{-\lambda\psi}(\sin\lambda\psi)H_e$$

$$= -2H_e\left(\frac{1}{t^{3/2}}\right)(r_2)^{1/2}e^{-\lambda\psi}\left[\left\{3\left(1-\nu^2\right)\right\}^{1/4}\cos\lambda\psi \pm \frac{3\nu}{\left\{3\left(1-\nu^2\right)\right\}^{1/4}}\sin\lambda\psi\right] \tag{49b}$$

7. Analytical observations

7.1. Effect of M_e

The magnitudes of the stresses due to M_e (both meridional and hoop) are not dependant on the principal radii r_1 and r_2 (and hence the parameters a and b) of the elliptic torus. For a given applied M_e, the magnitudes of the induced shell stresses only depend on the thickness t of the shell. This total lack of dependence on the elliptic parameters a and b is a surprising result.

It means that for the same moment M_e applied at the inner and outer edges of the semi-elliptic toroidal shell, the peak values of the induced shell stresses will be the same. However, the rate of decay of the stresses with distance from the respective shell edge, as well as the wavelength of the oscillations of the variation, will not be the same, because the value of the shell slenderness parameter λ (which governs both the rate of decay and the wavelength of the oscillations) at the outer edge differs from that at the inner edge – see Eq. (9).

7.2. Effect of H_e

The magnitudes of the stresses due to H_e (both meridional and hoop) not only depend on the shell thickness t, but more significantly, are directly proportional to $\sqrt{r_2}$. Now $r_2 = A + a$ for the outer edge of the semi-elliptic toroidal shell, and $r_2 = A - a$ for the inner edge (see Eqs. (3b) and (4b)). It therefore follows that, for the same horizontal shear force H_e applied at the inner and outer edges of the semi-elliptic toroidal shell, the peak values of the induced shell stresses on the outer side of the torus will differ from those on the inner side, since the r_2 values differ; the outer side will experience larger stresses than the inner side.

We also observe that only the parameters A and a of the elliptic toroid (but not b) have an influence on the peak values of the stresses due to H_e. The rate of decay of stresses with distance from the shell edge, as well as the wavelength of the oscillations, will also be different between the outer and inner sides, owing to the different values of λ.

For H_e, we may write the stresses for the outer and inner edges more explicitly as follows:

Outer edge

$$\sigma_\phi = \mp \frac{6H_e}{\left\{3\left(1-\nu^2\right)\right\}^{1/4}}\left(\frac{1}{t^{3/2}}\right)(A+a)^{1/2}e^{-\lambda\psi}\sin\lambda\psi \tag{50a}$$

$$\sigma_\theta = -2H_e\left(\frac{1}{t^{3/2}}\right)(A+a)^{1/2}e^{-\lambda\psi}\left[\left\{3\left(1-\nu^2\right)\right\}^{1/4}\cos\lambda\psi \pm \frac{3\nu}{\left\{3\left(1-\nu^2\right)\right\}^{1/4}}\sin\lambda\psi\right] \tag{50b}$$

Inner edge

$$\sigma_\phi = \mp \frac{6H_e}{\left\{3\left(1-\nu^2\right)\right\}^{1/4}}\left(\frac{1}{t^{3/2}}\right)(A-a)^{1/2}e^{-\lambda\psi}\sin\lambda\psi \tag{51a}$$

$$\sigma_\theta = -2H_e\left(\frac{1}{t^{3/2}}\right)(A-a)^{1/2}e^{-\lambda\psi}\left[\left\{3\left(1-\nu^2\right)\right\}^{1/4}\cos\lambda\psi \pm \frac{3\nu}{\left\{3\left(1-\nu^2\right)\right\}^{1/4}}\sin\lambda\psi\right] \tag{51b}$$

7.3. Comparisons with cylindrical and spherical shell solutions

Not surprisingly, the derived theoretical results for the elliptic toroidal shell are quite similar to those for the bending of a circular cylindrical shell, and for the bending of a non-shallow spherical shell when use is made of the Geckeler approximation [2,3]. Both of these problems also result in a fourth-order governing differential equation of the same form as Eq. (8), with a general solution of the same form as Eq. (10) or Eq. (11).

Looking at the expressions for N_θ, V, δ and M_ϕ (Eqs. (14), (15), (17) and (18) respectively), and replacing $r_1\,d\phi$ (for the curved meridian) by dx (for the cylindrical shell), one can transform the results for the elliptic–toroidal shell to those for a cylindrical shell. However, the cylindrical-shell model will not exactly replicate the behaviour of the toroid, since dx (parallel to the axis of revolution) is only an approximation for the real $r_1\,d\phi$, an approximation that is very good in the neighbourhood of $\phi = \pm\pi/2$ (errors are of the order of $\psi^2/6$, where ψ is the angle from the edge), and that becomes better as r_1 becomes larger, and exact as r_1 approaches infinity. When r_1 reaches infinity, the r_2 for the toroidal shell becomes the radius of the cylinder. If one wanted to use the cylinder solution to approximate the behaviour of the elliptic toroidal shell in the equatorial zones, the equivalent cylindrical shells for the outer and inner edges of the semi-elliptic toroid are the two cylinders which are tangential to the elliptic toroid at the extrados ($r_2 = A + a$) and the intrados ($r_2 = A - a$).

Alternatively, one may replace the elliptic toroidal shell with the equivalent spherical shell in the vicinity of the equatorial plane, and then use the Geckeler approximation. The equivalent spherical shells for the outer and inner edges of the semi-elliptic toroid are the two spheres which are tangential to the elliptic torus at the extrados and the intrados; these spheres are of radii $A + a$ and $A - a$ respectively.

For the outer edge of the elliptic toroid, the spherical-shell solution is a better approximation of the stress distribution in the elliptic toroid than the cylindrical-shell solution (the spherical surface and the elliptic–toroidal surface have the same value of r_1 at their tangent circle), but for the inner edge of the elliptic toroid, the cylindrical-shell approximation is better than the spherical-shell solution, owing to the inability of the sphere to model the meridional curvature of the elliptic torus on its inner side (the

spherical surface and the elliptic–toroidal surface have different *magnitudes* of r_1 at their tangent circle, and the *signs* of the curvature are also different).

8. Numerical results

As an example, consider a semi-elliptical toroidal shell with the parameters

$a = 10$ m; $b = 20$ m; $A = 30$ m; $t = 0.05$ m; $E = 200 \times 10^9$ N/m^2; $\nu = 0.3$

These parameters are possible proportions for a subsea marine observatory of circular plan shape, where the overall structural diameter is 80 m and the height is 40 m. The principal radii of curvature and shell slenderness parameters at the two edges follow from Eqs. (3), (4) and (9):

Outer edge: $r_1 = 40$ m; $r_2 = 40$ m; $\lambda = 36.3568$

Inner edge: $r_1 = -40$ m; $r_2 = 20$ m; $\lambda = 51.4163$

A bending moment $M_e = 100$ kNm/m is first applied at both the outer shell edge and the inner shell edge. The variations of meridional and hoop stresses with the angular coordinate ψ from the shell edge are given by Eqs. (48), which apply for both the outer edge and the inner edge, but using the λ value applicable for the edge in question. The arc length s (in metres) from the shell edge is simply given by $s = |r_1|\psi = 40\psi$, where angle ψ is in radians. Based on the theoretical formulation that has been developed in this paper, Fig. 4(a) shows plots of meridional and hoop stresses versus distance s from the *outer* edge, while Fig. 5(a) shows plots of meridional and hoop stresses versus distance s from the *inner* edge.

As a means for validating the theoretical results, a finite-element modelling of the semi-elliptic toroidal shell using the FEM programme ABAQUS [39] was performed, for an edge loading of

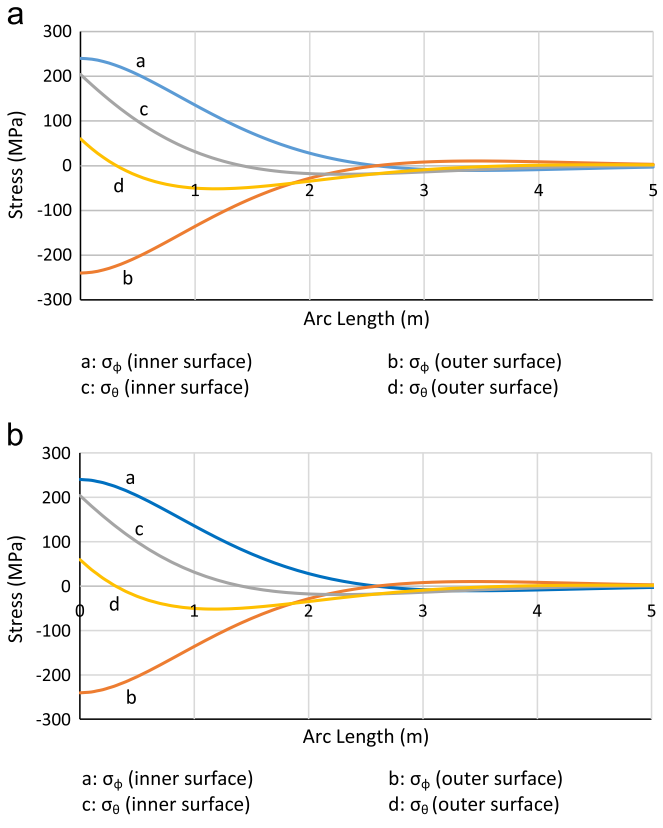

Fig. 4. Application of M_{e1} at the outer edge: (a) analytical results; (b) FEM results.

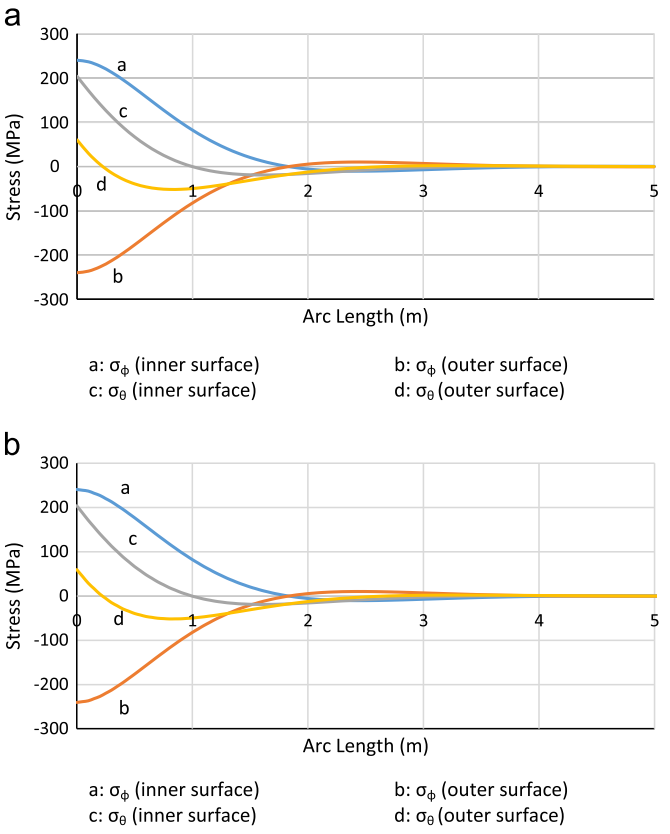

Fig. 5. Application of M_{e2} at the inner edge: (a) analytical results; (b) FEM results.

100 kNm/m. Two-node axisymmetric shell elements were employed throughout, with the element lengths kept at 0.05 m (very fine mesh) throughout in order to ensure accurate modelling of the rapidly varying bending-disturbance stresses in the edge zones. The FEM results are shown in Fig. 4(b) for the outer edge and Fig. 5(b) for the inner edge.

For the same shell, a horizontal shear force $H_e = 100$ kN/m is next applied at both the outer shell edge and the inner shell edge. The variations of meridional and hoop stresses with the angular coordinate ψ from the shell edge are given by Eq. (50) for the outer edge and Eq. (51) for the inner edge. Based on the theoretical formulation that has been developed in this paper, Fig. 6(a) shows plots of meridional and hoop stresses versus distance s from the *outer* edge, while Fig. 7(a) shows plots of meridional and hoop stresses versus distance s from the *inner* edge. The corresponding FEM results are shown in Figs. 6(b) and 7(b).

Comparing the analytical results versus their FEM counterparts, it is noted that the agreement is excellent throughout. The curves are practically identical. The discrepancy is generally less than 1% for both the outer edge of the semi-elliptic toroid and the inner edge, and for both the application of M_e and the application of H_e. This is clearer from Table 1, where peak values of the analytical plots are compared with peak values of the FEM plots; theoretical values and FEM values are almost identical. Owing to the fineness of the FEM mesh that was adopted (further refinement of the mesh did not change the results by more than 0.1%), the FEM results may be taken as exact for practical purposes. The achieved agreement of over 99% between the analytical and FEM results leads us to conclude that the proposed theoretical formulation for the equatorial bending of prolate elliptic toroidal shells, while approximate, is a very accurate and effective means for quantifying edge effects in regions bordering the extrados and intrados of such shells. This is a finding of significant practical importance.

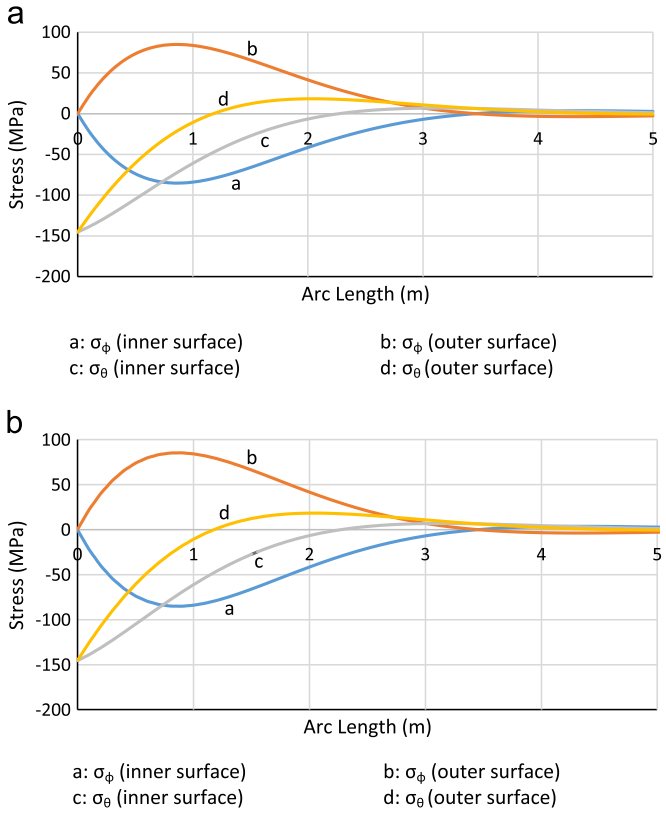

Fig. 6. Application of H_{e1} at the outer edge: (a) analytical results; (b) FEM results.

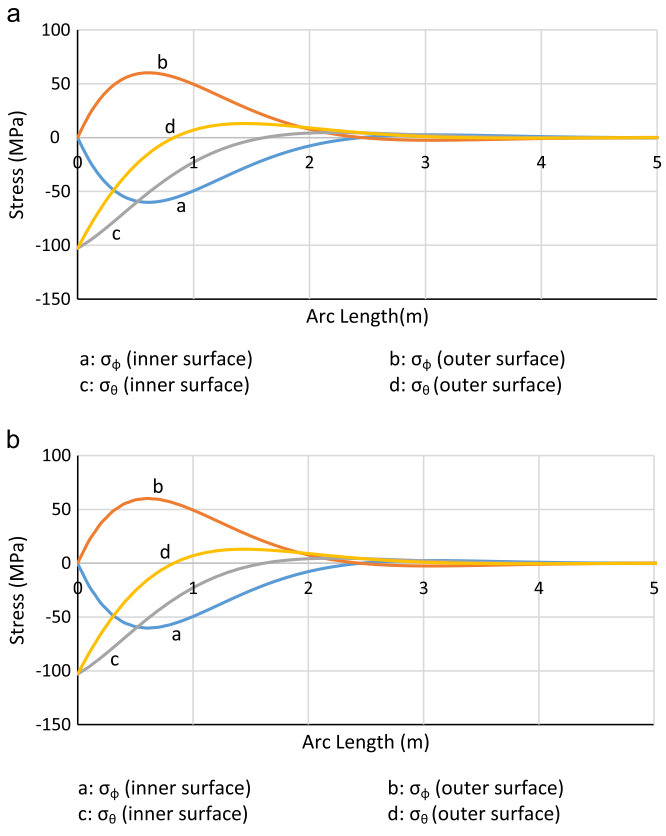

Fig. 7. Application of H_{e2} at the inner edge: (a) analytical results; (b) FEM results.

Comparing the two edges of the semi-elliptical toroid, and consistent with the analytical predictions, it is seen that the effects of H_e are larger on the outer side of the toroid (owing to the larger value of r_2 there). It is also observed that the bending disturbance decays more quickly on the inner side of the toroid (owing to the larger value of λ there).

9. Concluding remarks

The exact differential equations for the axisymmetric bending of elliptic toroidal shells are complex and difficult to solve analytically, since the coefficients of these equations are themselves complicated functions of the independent variable ϕ. For the estimation of bending effects in the mid-level regions of the prolate elliptical toroid ($b > a$), a simplication of the Reissner–Meissner equations has been proposed in this paper. This takes advantage of (i) the rapidly decaying character of edge effects, (ii) the slow rate of change of r_1 and r_2 (principal radii of curvature of the shell) in these regions of the toroid, and (iii) the fact that $\cot\phi \approx 0$ in the vicinity of the equatorial plane.

The relevant formulation for this approach has been developed, and closed-form expressions derived for shell stresses in the edge zones due to arbitrary bending moments M_e and horizontal shearing forces H_e applied at the outer and inner edges of the shell. The obtained closed-form results are surprisingly simple, yet capable of modelling mid-side edge effects with very high accuracy. For the example that was considered, errors were less than 1%.

By examining the final form of the analytical results, it has been observed that the magnitude of the stresses due to an edge bending moment M_e applied at the equatorial level is practically independent of the characteristic parameters a, b and A of the elliptic toroid, while that of the stresses due to a horizontal edge shear H_e is dependant on a and A (but not b). Thus the effects of a given action H_e are larger on the outer side of the toroid (owing to the larger value of r_2 there). It has been found that the effects of both M_e and H_e (which constitute the bending disturbance) decay more quickly on the inner side of the toroid, owing to the larger value of λ there. This finding is not obvious, since surfaces of negative Gaussian curvature (such as we find on the inner side of the torus) may exhibit more extensive propagation of edge effects [1].

Although arbitrary values of $M_e = 100$ kNm/m and $H_e = 100$ kN/m were assigned to the toroidal edges for the purposes of studying the ensuing stress distributions within the shell, in a real problem, the actual values of M_e and H_e depend on the loading acting over the surface of the shell and the boundary conditions prevailing at the shell edge; M_e and H_e are usually evaluated by imposing conditions of compatibility of deformations at the shell edge, when the effects of the membrane solution for a particular type of loading are considered simultaneously with the general effects of M_e and H_e, as developed in the present paper.

In particular, for elliptic toroidal vessels subjected to external or internal hydrostatic liquid pressure, the theoretical formulation that has been developed will be useful in providing an accurate estimate of stresses and deformations in the vicinity of (i) any mid-side discontinuities of the shell (such as discontinuities in shell thickness), (ii) axisymmetric vertical supports located at the mid-sides of the vessel, or (iii) the junction of the thin shell wall with an external ring stiffener or an internal plate deck located in the equatorial plane. A calculation of the deformed shape of the shell midsurface prior to the onset of elastic buckling, which this formulation will facilitate, can afford valuable insights on the likely mode of first buckling.

Table 1
Comparison of analytical (ANA) versus finite-element method (FEM) results.

	σ_ϕ (inner surface) N/mm^2		σ_ϕ (outer surface) N/mm^2		σ_θ (inner surface) N/mm^2		σ_θ (outer surface) N/mm^2	
	ANA	FEM	ANA	FEM	ANA	FEM	ANA	FEM
M_{e1} (outer edge)	240.0	240.3	−240.0	−240.3	204.2	204.1	60.2	59.9
M_{e2} (inner edge)	240.0	240.6	−240.0	−240.6	204.2	204.0	60.2	59.7
H_{e1} (outer edge)	−85.0	−85.1	85.0	85.1	−145.4	−145.6	−145.4	−145.4
H_{e2} (inner edge)	−60.2	−60.3	60.2	60.3	−102.8	−103.0	−102.8	−102.7

Acknowledgement

This work has been undertaken within the framework of a research programme funded by the National Research Foundation of South Africa.

References

[1] V.V. Novozhilov, Thin Shell Theory, Wolters-Noordhoff, Groningen, 1970.
[2] W. Flugge, Stresses in Shells, Springer-Verlag, Berlin, 1973.
[3] A. Zingoni, Shell Structures in Civil and Mechanical Engineering, Thomas Telford Publishing, London, 1997.
[4] E.H. Baker, L. Kovalevsky, F.L. Rish, Structural Analysis of Shells, McGraw-Hill, New York, 1972.
[5] S.P. Timoshenko, S. Woinowsky-Krieger, Theory of Plates and Shells, McGraw-Hill, New York, 1959.
[6] J.G. Teng, Buckling of thin shells: recent advances and trends, Appl. Mech. Rev.: Trans. ASME 49 (1996) 263–274.
[7] L.A. Godoy, E.M. Sosa, Localized support settlements of thin-walled storage tanks, Thin Walled Struct. 41 (2003) 941–955.
[8] R.C. Jaca, L.A. Godoy, F.G. Flores, J.G.A. Croll, A reduced stiffness approach for the buckling of open cylindrical tanks under wind loads, Thin Walled Struct. 45 (2007) 727–736.
[9] E.M. Sosa, L.A. Godoy, Challenges in the computation of lower-bound buckling loads for tanks under wind pressures, Thin Walled Struct. 48 (2010) 935–945.
[10] L. Chen, J.M. Rotter, C. Doerich, Buckling of cylindrical shells with stepwise variable wall thickness under uniform external pressure, Eng. Struct. 33 (2011) 3570–3578.
[11] J.M. Rotter, H. Schmidt (Eds.), Buckling of steel shells: European design recommendations 5th ed., European Convention for Constructional Steelwork, Brussels, 2013.
[12] G.C.M. Chan, A.S. Tooth, J. Spence, A study of the buckling behaviour of horizontal saddle supported vessels, Thin Walled Struct. 30 (1998) 3–22.
[13] P. Jasion, K. Magnucki, Elastic buckling of horizontal barrelled shells filled with liquid: numerical analysis, Thin Walled Struct. 52 (2012) 117–125.
[14] K. Magnucki, P. Jasion, Analytical description of pre-buckling and buckling states of barrelled shells under radial pressure, Ocean Eng. 58 (2013) 217–223.
[15] B.S. Golzan, H. Showkati, Buckling of thin-walled conical shells under uniform external pressure, Thin Walled Struct. 46 (2008) 516–529.
[16] A.A. El Damatty, E.G. Marroquin, M. El Attar, Behaviour of stiffened liquid-filled conical tanks, Thin Walled Struct. 39 (2001) 353–373.
[17] G. Hafeez, A.M. El Ansary, A.A. El Damatty, Stability of combined imperfect conical tanks under hydrostatic loading, J. Constr. Steel Res. 66 (2010) 1387–1397.
[18] J. Blachut, P. Smith, Buckling of multi-segment underwater pressure hull, Ocean Eng. 35 (2008) 247–260.
[19] P. Jasion, K. Magnucki, Elastic buckling of Cassini ovaloidal shells under external pressure: theoretical study, Arch. Mech. 67 (2015) 1–14.
[20] P. Jasion, K. Magnucki, Elastic buckling of clothoidal-spherical shells under external pressure: theoretical study, Thin Walled Struct. 86 (2015) 18–23.
[21] A. Zingoni, Stresses and deformations in egg-shaped sludge digesters: membrane effects, Eng. Struct. 23 (2001) 1365–1372.
[22] A. Zingoni, Stresses and deformations in egg-shaped sludge digesters: discontinuity effects, Eng. Struct. 23 (2001) 1373–1382.
[23] A. Zingoni, Discontinuity effects at cone-cone axisymmetric shell junctions, Thin Walled Struct. 40 (2002) 877–891.
[24] A. Zingoni, Parametric stress distribution in shell-of-revolution sludge digesters of parabolic ogival form, Thin Walled Struct. 40 (2002) 691–702.
[25] A. Zingoni, B. Mokhothu, N. Enoma, A theoretical formulation for the stress analysis of multi-segmented spherical shells for high-volume liquid containment, Thin Walled Struct. 87 (2015) 21–31.
[26] V. Konopioska, W. Pietraszkiewicz, Exact resultant equilibrium conditions in the non-linear theory of branching and self-intersecting shells, Int. J. Solids Struct. 44 (2007) 352–369.
[27] W. Pietraszkiewicz, V. Konopioska, On unique kinematics for the branching shells, Int. J. Solids Struct. 48 (2011) 2238–2244.
[28] J.G. Teng, F. Chan, Elastic buckling strength of T-section transition ringbeams in steel silos and tanks, J. Constr. Steel Res. 56 (2000) 69–99.
[29] F. Khalili, H. Showkati, T-ring stiffened cone cylinder intersection under internal pressure, Thin Walled Struct. 54 (2012) 54–64.
[30] A. Zingoni, Liquid-containment shells of revolution: a review of recent studies on strength, stability and dynamics, Thin Walled Struct. 87 (2015) 102–114.
[31] C.R. Calladine, Theory of Shell Structures, Cambridge University Press, Cambridge, 1983.
[32] W.J. Sutcliffe, Stress analysis of toroidal shells of elliptical cross-section, Int. J. Mech. Sci. 13 (11) (1971) 951–958.
[33] G.D. Galletly, Elastic buckling of complete toroidal shells of elliptical cross-section subjected to uniform internal pressure, Thin Walled Struct. 30 (1998) 23–34.
[34] A. Combescure, G.D. Galletly, Plastic buckling of complete toroidal shells of elliptical cross-section subjected to internal pressure, Thin Walled Struct. 34 (1999) 135–146.
[35] D. Redekop, Buckling analysis of an orthotropic elliptical toroidal shell. In: Proceedings of the ASME Pressure Vessels & Piping Conference 2009, (Design & Analysis), 2009; vol. 3, pp. 33–40.
[36] G. Yamada, Y. Kobayashi, Y. Ohta, S. Yokota, Free vibration of a toroidal shell with elliptical cross-section, J. Sound Vib. 135 (3) (1989) 411–425.
[37] B. Xu, D. Redekop, Natural frequencies of an orthotropic thin toroidal shell of elliptical cross-section, J. Sound Vib. 293 (2006) 440–448.
[38] H.J. Zhan, D. Redekop, Vibration, buckling and collapse of ovaloid toroidal tanks, Thin Walled Struct. 46 (2008) 380–389.
[39] ABAQUS Standard, Newark (California), Hibbit, Karlsson and Sorenson Inc, 1998.